Gadolinium-containing phosphatidylserine liposomes for molecular imaging of atherosclerosis

Andrei Maiseyeu,* Georgeta Mihai,* Thomas Kampfrath,* Orlando P. Simonetti,* Chandan K. Sen,[†] Sashwati Roy,* Sanjay Rajagopalan,* and Sampath Parthasarathy[1,†]

Davis Heart and Lung Research Institute* and Department of Surgery,[†] Ohio State University, Columbus, OH

Abstract Exteriorized phosphatidylserine (PS) residues in apoptotic cells trigger rapid phagocytosis by macrophage scavenger receptor pathways. Mimicking apoptosis with liposomes containing PS may represent an attractive approach for molecular imaging of atherosclerosis. We investigated the utility of paramagnetic gadolinium liposomes enriched with PS (Gd-PS) in imaging atherosclerotic plaque. Gd-PS-containing Gd-conjugated lipids, fluorescent rhodamine, and PS were prepared and characterized. Cellular uptake in RAW macrophages (fluorescent uptake of rhodamine) was studied on a fluorescence plate reader, while Gd-PS-induced alteration in T1 relaxivity was evaluated using a 1.5 T MRI scanner. RAW cells demonstrate PS-dependent uptake of across a range of concentrations (2, 6, 12, and 20%) in comparison to control liposomes with no PS (0%). In vivo performance of Gd-PS was evaluated in the ApoE$^{-/-}$ mouse model by collection of serial T1 weighted gradient echo MR images using an 11.7 T MRI system and revealed rapid and significant enhancement of the aortic wall that was seen for at least 4 h after injection. Gd-PS-enriched liposomes enhance atherosclerotic plaque and colocalize with macrophages in experimental atherosclerosis.—Maiseyeu, A., G. Mihai, T. Kampfrath, O. P. Simonetti, C. K. Sen, S. Roy, S. Rajagopalan, and S. Parthasarathy. Gadolinium-containing phosphatidylserine liposomes for molecular imaging of atherosclerosis. *J. Lipid Res.* 2009. **50:** 2157–2163.

Supplementary key words macrophages • apoptosis mimicking • cellular uptake • colocalization with macrophages • ApoE$^{-/-}$ mouse model

Molecular imaging approaches in atherosclerosis have the advantage of visualizing specific events that may be of relevance in the progression and complications of the disease (1, 2). Imaging strategies that allow visualization of inflammatory cells are particularly attractive in view of the fundamental role of this process in atherosclerosis (3). Macrophage identification strategies are particularly attractive for molecular imaging in light of their ubiquitous presence and positive correlation with complications of atherosclerosis. A number of different targeted contrast agents specific for macrophage proteins have been tested in atherosclerosis. In such approaches, the contrast strategy is typically paramagnetic gadolinium (Gd) chelates or iron (Fe) oxide particles and is passively incorporated to various carrier molecules. The carrier moieties by virtue of preferential uptake by, or delivery to, specific pathways or receptors of relevance to the macrophage allow for "high-payload" delivery of the contrast agent and facilitate imaging with adequate signal to background noise ratios. Examples of such approaches include HDL (4) and LDL (5) lipoproteins incorporating Gd, polyethyleneglycol (PEG) grafted immunomicels (6, 7), and liposome vesicles (8) conjugated to antibodies targeting the macrophage scavenger receptor. In general, these approaches have been shown to provide enhanced detection of macrophage-rich areas, allowing monitoring of macrophage-rich areas. Although these strategies are attractive, they do have several disadvantages, including considerable difficulties in preparation and handling, expense (e.g., antibodies), nonspecificity of targeting, and steric hinderances pertaining to the carrier moieties, such as PEG that may reduce targeted interaction of the antibody to sites of recognition (9, 10). It is well known that exteriorized phosphatidylserine (PS) residues present in apoptotic cells promote macrophage recognition by macrophage scavenger receptor/CD36 followed by rapid phagocytosis (11, 12). Accordingly, we hypothesized that mimicking apoptosis with liposomes containing PS may represent an attractive approach for molecular imaging of atherosclerosis.

This article is available online at http://www.jlr.org

Abbreviations: DOPE-Rho, phosphatidylethanolamine-Lissamine-Rhodamine B; Gd, gadolinium; Gd-DTPA-SA, Gd-diethylenetriamine-pentaacetic acid distearylamide; LDH, lactate dehydrogenase; MSR, macrophage scavenger receptor; NENH, normalized enhancement; PC, phosphatidylcholine; PEG, polyethyleneglycol; PG, phosphatidylglycerol; PS, phosphatidylserine; SNR, signal-to-noise ratio.

[1] To whom correspondence should be addressed.
e-mail: spartha@osumc.edu

Here, we describe a non-PEGylated, antibody-free, targeted contrast agent approach for macrophage imaging (**Fig. 1**).

MATERIALS AND METHODS

Reagents

Egg-phosphatidylcholine (PC), egg-phosphatidylglycerol (PG), brain-PS, and phosphatidylethanolamine-Lissamine-Rhodamine B (DOPE-Rho) were purchased from Avanti Polar Lipids (Alabaster, AL). Cholesterol and all other chemicals were obtained from Sigma-Aldrich (St. Louis, MO); Gd-diethylenetriaminepentaacetic acid distearylamide (Gd-DTPA-SA) was synthesized according References 13 and 14, RPMI 1640, FBS, and PBS were purchased from Cellgro Mediatech (Herndon, VA); and penicillin-streptomycin, glutamine, and sodium pyruvate were from Gibco/Invitrogen (Carlsbad, CA).

Paramagnetic liposomes

Liposomes were prepared by lipid film hydration (10, 12, 14). Briefly, solutions of lipids in chloroform were mixed and solvent was evaporated in vacuo. The molar composition of vesicles was 28.95% to 18.95% PC, 28.95% to 18.95% PG, 0% to 20% PS, 0.1% or 0.5% DOPE-Rho, 35% cholesterol, and 7% Gd-DTPA-SA. The vesicles containing different concentrations of PS were made by decreasing of amount of PC and PG simultaneously to accommodate increases in PS, while amount of DOPE-Rho, cholesterol, and Gd-DTPA-SA remained constant. Residue was pumped for 2–3 h and hydrated with 1 ml of HEPES buffer (20 mM HEPES and 135 mM NaCl, pH 7.2) at 55°C. After vigorous vortexing, resulting liposome suspension was passed through 400 and 200 nm Nucleopore membranes (21×) using mini extruder (Avanti Polar Lipids). Fluorescent paramagnetic liposomes always contained 0.1 mol% and 0.5 mol% DOPE-Rho for in vitro and in vivo experiments, respectively, and 7% of Gd-DTPA-SA. Control liposomes contained the same kind and amount of lipids except PS. The absence of later was compensated for by an equal amount of PG. For all cell studies, liposomes were prepared in concentration 10 mg/ml total lipid, and for in vivo MRI experiments, 25 mg/ml of total lipid concentration was used. The liposome particle size was determined using Dynamic Light Scattering on Nano S Zetasizer (Malvern Instruments). Liposomes had mean size of 230 nm with a narrow size distribution. Lipids concentration was determined by the Stewart method (15).

Cell culture

RAW 264.7 macrophages were obtained from American Type Culture Collection (Manassas, VA). Cells were cultured in complete RPMI media containing 10% FBS, 1% penicillin-streptomycin, 1% glutamine, and 1% sodium pyruvate at 37°C, 5% CO_2. For fluorescent and cytoxicity studies, cells were plated in opaque 96-well plates with 10^4 cells per well. After 24 h of incubation, the cells were washed with PBS (1×), and each well was incubated with 100 µl phenol red-free medium containing 50 µg of appropriate liposome formulation or Magnevist (as a control in cytoxicity experiments). After 12 h, cells were washed with prewarmed PBS (2×, 100 µl) and assayed on fluorescence plate reader (Victor V; Perkin-Elmer). For in vitro MRI experiments, cells were placed in 300 cm² culture flasks (8×10^6 cells per flask, 80 ml of media) and after 24 h of incubation, the media were removed and replaced with fresh media. Liposomes (1 ml, 40 mg/ml of lipids) were then added and gently swirled, and cells were incubated in a wet atmosphere at 37°C, 5% CO_2 for 12 h. Then, the old media were aspirated off and cells were washed twice with 80 ml of prewarmed PBS. Next, deionized water was added (50 ml per flask), and flasks were agitated on an orbital shaker for 1 h. Resulting suspension of cell lysate was transferred into 50 ml Falcon tubes and centrifuged at 1,500 g for 5 min. Pellet was isolated, frozen in dry ice, and lyophilized. Resulting dry powder was reconstituted by sonication in 1 ml of 10% Triton X-100. Mixture was transferred to Eppendorf tubes and imaged in a 1.5 T MRI scanner (Avanto, Siemens, Erlangen, Germany).

Cellular toxicity assay

Cells were prepared as indicated above (cell culture section), and the same liposomes but containing no fluorescent lipids were added to each well at three different doses: 6 µg of liposomes containing 0.1 µg of Gd, 60 µg of liposomes containing 1.0 µg of Gd, and 120 µg of liposomes containing 2.0 µg of Gd. Two controls were used: the same amount of liposomes without Gd-DTPA-SA and Magnevist, diluted with HEPES buffer corresponding to Gd concentrations of 0.1, 1.0, and 2.0 µg per well. The lactate dehydrogenase (LDH) assay was carried out using the CytoTox-ONE homogeneous Membrane Integrity Assay (Promega, Madison, WI)

Microscopy

Cells were grown in 6-well plates in conditions described above. Cultured macrophages were treated with fluorescent liposomes at concentration 0.45 mg total lipids per well. After an appropriate incubation period, cells were fixed by the addition of cold 2% paraformaldehyde and fluorescence was analyzed. Optical imaging of cells treated with fluorescent liposomes was performed on a Nikon Eclipse FN1 microscope (Japan) using a 40×/0.80 W water immersed objective. The data were processed using Metamorph software (version 7.1.2.0; Metamorph, Downingtown, PA).

Confocal fluorescence microscopy and immunohistochemistry

At the end of the MRI experiment, mice were euthanized, and the aortas were immediately removed and embedded in optical cutting temperature compound. Sectioned abdominal aortas (8 µM) were immersed into ice-cold ethanol for 5 min and then air dried and rehydrated with PBS. After treatment with 0.02% Triton X-100 and successive washing with PBS, slides were blocked with goat serum and then incubated with FITC-conjugated rat
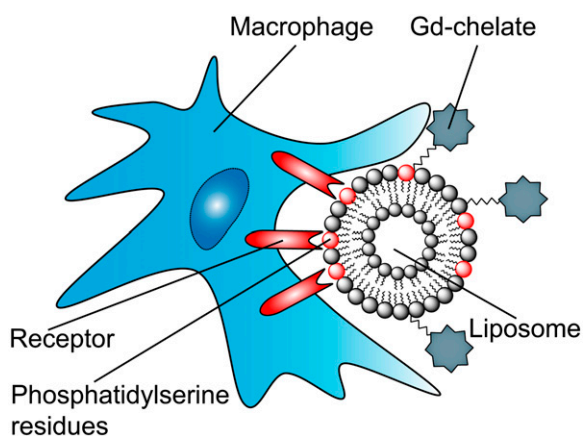

Fig. 1. Schematic representation of hypothesis. PS-enriched liposomes are recognized by macrophages and thereby can serve as targeted contrast agents to macrophage-rich areas, such as atherosclerotic plaque.

anti-mouse CD68 monoclonal antibody (clone fa-11; Serotech, Raleigh, NC).

Following washing, slides were incubated with 10 μM Hoechst 33342 (Invitrogen, Carlsbad, CA) and mounted. Tissue images were collected using an inverted Zeiss LSM 510 confocal microscope equipped with Argon (458, 477, 488, and 514 nm), green HeNe (543 nm), and red HeNe (633 nm) lasers. For Hoechst 33342 fluorescence, a titanium sapphire two-photon laser was used. Objective used was C-Apochromat ×63/1.2 numerical aperture water immersion (Zeiss). Data were analyzed using Zeiss LSM 510 Meta and Image Browser software.

Animals

Nine 32 week old ApoE$^{-/-}$-knockout mice were used for in vivo MRI experiments. Six animals were subjected to treatment with Gd-PS, while three mice were in control group and received control contrast agent. The animals were fed a normal chow diet. Contrast agents were administered intravenously at a dose of 0.1 mmol Gd/kg. All animals were treated according to the Principles of Laboratory Animal Care of the National Society or Medical Research and the Guide for the Care and Use of Laboratory Animals. (16) The experimental protocol was approved by the Institutional Animal Care and Use Committee.

MRI

In vivo MRI scans were performed using an 11.7 T Bruker NMR System (Billerica, MA) with a 52 mm inner diameter vertical bore and a 300 G/cm gradient strength. Mice were anesthetized with inhaled isoflurane (maintenance: 1.5–2%) and fixed head-up with paper tape in a 32 mm transmit/receive birdcage coil. No respiratory or cardiac gating was used as the imaged abdominal area is not significantly affected by respiratory or cardiac motion artifacts. The abdominal aorta and the kidney, which were used as the main anatomical landmark, were initially identified by acquiring 25 0.5-mm coronal slices using a two-dimensional T1 weighted spin echo localizing sequence (TR/TE = 528/10.2 ms, scan time = 2:20 min). A gradient echo T1 weighted sequence with acquisition parameters optimized to depict the aortic wall was used to visualize the aortic wall pre- and postcontrast injection. Twelve two-dimensional, $0.1 \times 0.1 \times 0.5$ mm^3 transversal contiguous slices, with the top one placed just below kidney, were acquired using a gradient echo sequence (TR/TE = 316/3.7 ms, flip angle = 22, four averages, total scan time = 5:56 min). The anterior placement of a 7 mm arterial flow suppression axial slab allowed for delineation of the inner and better depiction of the outer arterial wall. After localization and acquisition of the precontrast scan, each mouse was taken out of the

magnet and while still placed in the birdcage coil holder was tail vein injected with contrast agent and immediately placed back in the magnet for the postcontrast scans. Each mouse was imaged for approximately 1.5–2 h after contrast administration using repetitive acquisitions of the 5:56 min gradient echo sequence. Just minutes before 4, 8, 12, and 24 h postcontrast, each mouse was anesthetized and placed back in the magnet, and a single MRI scan was acquired using the T1 weighted gradient echo sequence.

Image analysis

MR images were analyzed using ImageJ (NIH). For each mouse, four slices common to the all time points were identified by checking the shape and position of the spinal column. For each time point, the thickened aortic wall was identified, and one irregular 25–35 pixel region of interest, which covered the entire aortic wall, less the region next to vena cava, was hand drawn on each slice. Signal-to-noise ratio (SNR) of each region of interest was calculated as the average signal intensity divided by the standard deviation of the noise level. The SNRs of the four slices were averaged and displayed as a function of time to depict the time course of the signal intensity changes due to contrast uptake in the atherosclerotic wall. Percentage of normalized enhancement (NENH) was calculated by the formula: % NENH = 100 × (SNR_{post}/SNR_{pre}); SNR_{post} and SNR_{pre} are the SNRs obtained after and before contrast agent administration, respectively.

Statistics

All values in this article represent mean ± SD unless otherwise specified. One-way ANOVA methodology was used to compare multiple variables or time points with $P < 0.05$ representing statistically significant differences. A Bonferroni posthoc correction was used to assess differences between groups. All statistics were performed using GraphPad Prism (Version 4.0; GraphPad Software, La Jolla, CA).

RESULTS

Optimization of liposome formulations and evaluation of its T1 by MRI

Figure 2A represents chemical structure of the Gd-DTPA-SA complex used in the preparation of liposomal Gd complexes in our experiments. Preliminary studies were then performed to optimize liposomal lipid composition, which demonstrated that liposomes containing PC,
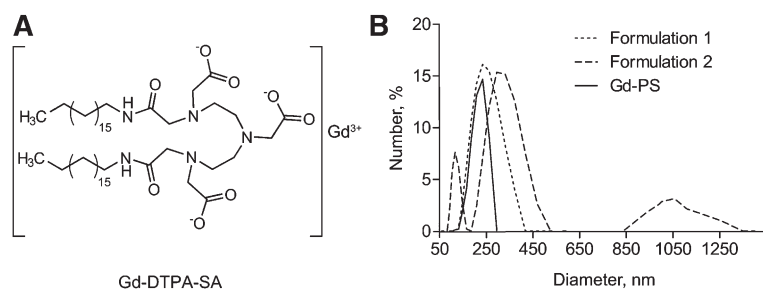

Fig. 2. Liposomal formulations: content and properties. A: Gd source: Gd-DTPA-SA complex was incorporated into liposomal lipid membranes. B: Size distribution of paramagnetic liposomes. Formulation 1 contained 29 mol% PC and PG, 2 mol% PS, 7 mol% Gd-DTPA-SA, 35 mol% cholesterol, and 0.1% of DOPE-Rho. Formulation 2 contained 58 mol% PC, 2 mol% PS, 7 mol% Gd-DTPA-SA, 35 mol% cholesterol, and 0.1% of DOPE-Rho. Gd-PS was formed from 22.95 mol% PC and PG, 12 mol% PS, 7 mol% Gd-DTPA-SA, 35 mol% cholesterol, and 0.1% of DOPE-Rho.

PG, and PS lipids were stable at all experimental conditions and could be prepared within a defined size range. Figure 2B depicts the results of particle size measurements for two formulations. Formulation 1 containing PC/PG liposomes was characterized by a limited size distribution, as opposed to liposomes formulated with PC and low PS concentrations (presumably secondary to significantly less surface charge interactions). We therefore used the PC/PG and PS preparations in all subsequent experiments (Fig. 2B legend provides the relative concentration of individual phospholipids).

Liposomes containing PC, PG, and PS were then incorporated with Gd-DTPA-SA along with the fluorescent dye Rhodamine B to allow for in vivo tracking. This composite formulation was used in all further experiments.

We then investigated the appropriate concentration of Gd-PS liposomes for our in vitro and in vivo MRI experiments. Liposomal formulations were prepared at 5–35 mM of lipids and contained 7% Gd-DTPA-SA. The 35 mM concentration of liposomes was used for the following reasons. Relatively low concentration of phospholipids allowed for rapid and easy liposome extrusion and was convenient for intravenous injection into the tail vein of mice using narrow gauge venous catheters. Additionally, volumes of 400–500 μl contained 0.1 mmol Gd/kg and represented the clinical dose of Gd most commonly used for cardiovascular MRI applications (17).

MRI experiments performed on freshly prepared Gd-PS at different concentrations were compared with the clinically used contrast agent Magnevist (Schering, Germany). **Table 1** provides the T1 relaxivities of various Gd-PS formulations where the lipid concentration was varied and compared with a Magnevist preparation containing an identical amount of Gd as the liposomes. As the T1 of Gd-PS (containing 35 mM of phospholipids) at 20 ms was roughly comparable to that of 3 μM Magnevist (T1 = 9 ms), these findings further additionally supported use of the 35 mM concentration of phospholipids for in vivo experiments (Table 1).

RAW macrophages demonstrate PS-dependent cellular uptake of Gd liposomes

Our next goal was to understand the optimal concentration of PS for successful targeting to macrophages. Recent studies suggest that PS exposed in apoptotic cells is crucial in the recognition and uptake (18). To demonstrate that Gd-PS and its recognition by macrophages may be superior when compared with conventional PC liposomes, PC liposomes and Gd-PS containing a range of PS concentrations (mol: 2, 6, 12, and 20%) were incubated with cultured RAW macrophages. All liposomal formulations had

TABLE 1. T1 values of Gd-PS and relative controls

Sample Concentration	T1, ms
Water	2,536 ± 11
5 mM Gd-PS (0.4 μM Gd)	274 ± 0.53
35 mM Gd-PS (3 μM Gd)	20 ± 0.63
0.4 μM Magnevist	64 ± 0.03
3 μM Magnevist	9 ± 0.14

fluorescent DOPE-Rho and paramagnetic Gd-DTPA-SA. Cellular uptake was visualized by fluorescent microscopy after 12 h of incubation time. Images of labeled cells are presented in **Fig. 3**. Cells treated with PC liposomes demonstrated insignificant uptake when compared with Gd-PS with concentrations of PS >2%. Cells exposed to Gd-PS, at PS concentrations >2%, assimilated more fluorescent material up to PS concentrations of 12%, with a decrease in uptake at high PS concentrations (20%).

In vitro validation of Gd-PS uptake and safety

The effect of Gd-PS uptake by cells on T1 relaxivity was further assessed in RAW macrophages. Control liposomes with no PS (0%) and the same Gd-PS liposomes at various PS concentrations used in prior experiments were prepared and incubated with RAW cells for 12 h. Cell lysates were prepared and imaged on a 1.5T MRI scanner using an inversion recovery T1 weighted spin-echo sequence (TR/TE = 1500/13.8, flip angle = 180, TI = 22–2750 ms). A decrease in T1 value was observed in cells treated with Gd-PS compared with controls incubated with PC liposomes, indicating an effect on longitudinal T1 relaxation time with Gd-PS (**Fig. 4A, Table 2**). There was no further shortening in T1 observed beyond the 2% PS concentration. Fig. 4B depicts quantitative results on uptake of Gd-PS using a fluorescent plate reader with the results expressed as relative fluorescence units. The disparity between T1 shortening and fluorescent uptake suggests that Gd uptake or localization in the cell membrane may not depend on the same mechanisms that facilitate PS uptake or that the concentrations of Gd required to further decrease T1 relaxation may necessitate large increases in Gd not achievable with our preparations. Since the maximum uptake by fluorescence was noted at the 12% PS data point, the corresponding formulation was chosen for further in vivo MRI experiments.

In vitro toxicity of Gd-PS was compared with two controls: liposome formulation without paramagnetic material (Gd-DTPA-SA) and Magnevist. The first control (PS-Lipo) contained the 12% PS incorporated in liposomes without Gd, while Magnevist preparation contained an identical amount of Gd as Gd-PS. Cells were then cultured as indicated in Materials and Methods, and three different doses of Gd-PS and both controls were applied to
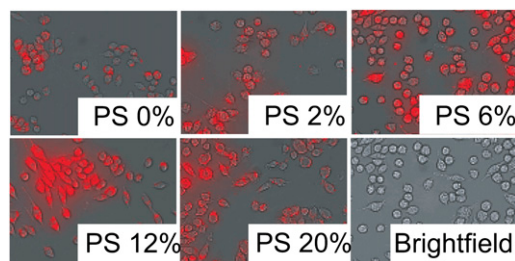

Fig. 3. Fluorescent microscopy images of treated by Gd-PS cells. Adherent raw cells were incubated with PS liposomes containing 0.1% rhodamine-phospholipid dye. PC liposomes were used as a reference. Selective to Gd-PS uptake by raw macrophages can be visualized in comparison to control PC liposome-treated cells
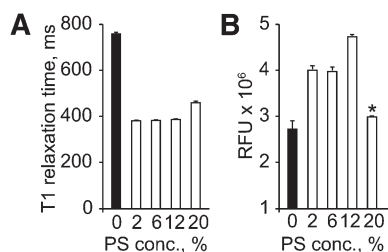
Fig. 4. Uptake of PS-enriched liposomes across a range of concentrations (2, 6, 12, and 20%) in comparison to control liposomes with no PS (0%). A: Raw cells were treated with Gd-PS liposomes, and T1 relaxivities of cell lysate pellets were measured at 1.5 T after 12 h of incubation. There was a significant drop in T1 values of Gd-PS when compared with control showed gadolinum uptake induced by PS-containing liposomes, but not by PC liposomes. B: Treatment of cultured cells with the same formulations of Gd-PS and control for 12 h and following fluorescent assay on the fluorescence plate reader revealed the maximum uptake at 12% PS. The obtained relative fluorescence unit (RFU) values represent an excellent concordance with T1 assay and fluorescence microscopy studies (Fig. 3). *P < 0.05.

them with following the incubation and measurement of the number of nonviable cells. LDH release from all treated cells was minimal at 0.1 μg Gd (6 μg lipids) and almost without any difference between Gd-PS and controls (**Fig. 5**). There was little difference in toxicity between all three doses for PS-Lipo. This suggests that the toxicity may be related only to Gd in the sample. This also can be considered as normal cell growth and proliferation taking place in spite of presence of phospholipids. At 1.0 μg Gd (60 μg lipids), Gd-PS showed less toxic effect than Magnevist; however, at the higher concentrations, they both resulted in comparable cytotoxcity.

In vivo MRI validation of Gd-PS liposomes as contrast agent strategy

In vivo MRI imaging was performed in ApoE$^{-/-}$ mice using a gradient echo approach (see Materials and Methods). The abdominal aorta was imaged axially starting below the kidney to the aortic bifurcation using a gradient echo sequence, before and after in vivo administration of Gd-PS or control liposomes. The presence of plaque in all the animals was confirmed following euthanizing, and representative Hematoxylin and Eosin (H and E) staining depicting plaque are provided as part of the figure as well. **Figure 6A** depicts representative axial MRI images to assess contrast opacification with Gd-PS, while Fig. 6B represents representative images following nonPS liposomes containing Gd. Enhancement of plaque seen in control nonPS liposomes was seen at 60 min postcontrast administration, with prolonged retention of signal intensity at 8 h after

TABLE 2. T1 values resulting from Gd-PS-treated cells

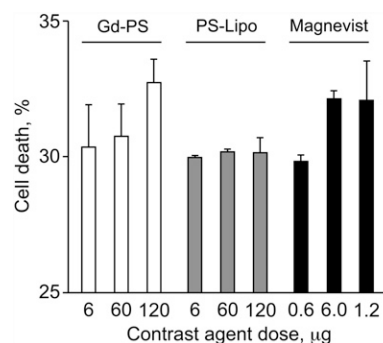| Liposome Formulation Containing PS (%)	T1, ms
0	771.56 ± 3.23
2	387.70 ± 0.60
6	388.99 ± 0.58
12	392.65 ± 2.33
20	467.29 ± 4.78

Fig. 5. LDH assay. Assay results calculated to show percentage of cytoxicity as a result of added Gd-PS and comparison to liposomal formulation without paramagnetic Gd-DTPA-SA (PS-lipo). For reference, cells were treated with Magnevist containing the same concentration of Gd as Gd-PS liposomes.

injection. Increase in signal was discernible at 10 min, with both agents probably related to a first pass perfusion effect, followed by a decrease probably related to redistribution and then a steady state phase related to equilibration. Signal decreased rapidly from 55 min onward in the control liposomes, while the decrease in the Gd-PS was gradual beyond 120 min with obvious retention in the vessel wall at 8 h. In contrast, the signal intensity in the control liposomes was no different from the precontrast phase (100% NENH; Fig. 6C).

Colocalization of macrophages and Gd-PS in vivo

As evidence of colocalization atherosclerosis-associated macrophages with Gd-PS in vivo, we performed confocal fluorescence imaging on sectioned mice aortas. Abdominal aortas were removed and immunostained 24 h postcontrast injection. To localize atherosclerosis-derived macrophages, we used CD-68 FITC-conjugated antibody and Hoechst 33342 to show nuclei of cells. Fluorescently labeled Gd-PSs were visible in the peri-adventitial region (red fluorescence from rhodamine). The CD-68 staining indicated the presence of macrophages in the plaque area (green from FITC). Colocalization of rhodamine with some of the FITC appeared yellow and was detected primarily in the peri-adventitia (**Fig. 7**). The obtained images demonstrate in vivo delivery of Gd-PS to macrophage-rich areas. These results along with MRI data strongly support our central hypothesis of targeted macrophage behavior of Gd-PS in vivo.

DISCUSSION

In this study, we describe a novel approach to imaging macrophages using PS-containing liposomes. This approach resulted in significant enhancement of atherosclerotic plaque in vivo for a prolonged duration and demonstrates the feasibility of such an approach for molecular characterization of high-risk plaque. Liposomal composition can be easily adjusted by including different lipids into the vesicle double layer and allows for inclusion of paramagnetic material and fluorescence tags for in vivo
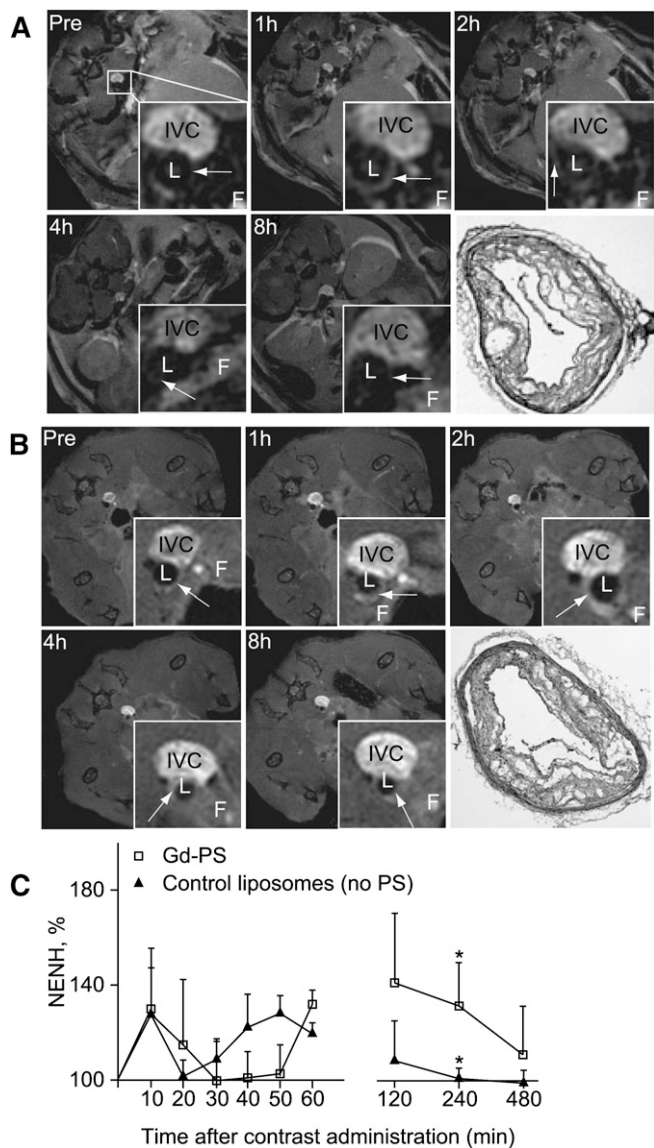
Fig. 6. Results of in vivo testing of Gd-PS on ApoE$^{-/-}$ knockout mouse model. Representative T1-weighted MR images prior to and after Gd-PS and control liposomes administration at different time points. Magnified areas of the region of interest are outlined in the insets. After injection, significant contrast enhancement appears in the plaque (white arrows) as shown in the insets of the aorta. Delineation of aortic wall after contrast enhancement is clearly improved. The bottom-right panels are the matched histopathological sections stained with H and E. The locations of the inferior vena cava (IVC), lumen (L), and abdominal fat (F) are indicated. A: MRI of atherosclerotic plaque with Gd-PS. B: Control imaging experiment with liposomes containing no PS. Maximum enhancement at 1 h and rapid disappearance of signal over next 2 h. C: NENH values of wall enhancement with Gd-PS and control liposomes without PS. *$P < 0.05$.

Fig. 7. Confocal microscopy images of ApoE$^{-/-}$ mouse abdominal aorta 24 h after injection of fluorescent paramagnetic liposomes Gd-PS. A: Red indicates rhodamine from Gd-PS accumulated in adventitia macrophage-rich areas. B: Macrophages associated CD68-FITC immunohistochemical stain (green). C: Nuclear stain Hoechst 33342 (blue) was used to localize nuclei. D: Overlay (yellow) proves Gd-PS liposomes were taken by macrophages. Bar = 20 μm.

monitoring of tissue/cell-specific delivery. In our approach, we used a simple route to prepare nonPEGylated liposomes containing a well-known lipophilic Gd chelate-Gd-DTPA-SA (13, 14) and fluorescent organic dye Rhodamine B to assess cellular uptake. Based on our studies, PS liposomes appear to be avidly taken up by macrophages. Our approach takes advantage of well-described pathways for PS-containing epitopes, as these are analogous to exte-
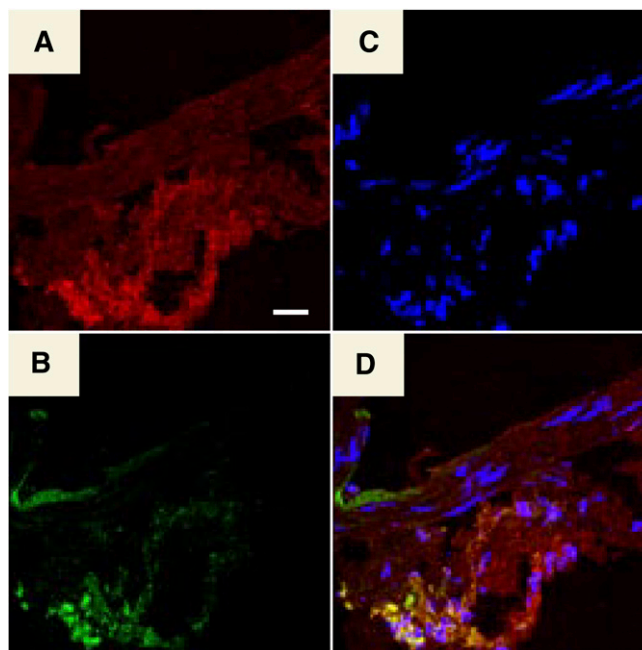
riorized PS residues as a consequence of apoptosis (11, 18, 19). We did not see significant decreases in T1 shortening beyond 2% PS, while we did see a continuing increase in fluorescent uptake of Gd-PS in our in vitro studies at least to the 12% PS concentration. This discordance in results using fluorescence and MRI-based measures may relate to potential differences in the measurements with MRI and fluorescence. Gd entry into the cell is gauged by changes in T1 values (an exponential variable), whereas changes in fluorescence measurements are typically linear over the ranges studied.

In our study, we obtained high-resolution images of plaque-containing regions of abdominal aorta at different time points. After injection of Gd-PS, significant enhancement of aortic wall was induced initially by blood flow bearing contrast agent (first pass enhancement). This was followed by a more gradual and sustained increase in signal at the later time points (>50 min), which likely represents targeted accumulation of paramagnetic material in the plaque macrophages as evidenced by our colocalization experiments. Our experiments comparing this with Gd-liposomes not containing PS clearly show that the presence of PS clearly allows accumulation of the contrast agent in the arterial wall. Although we did not study additional time points beyond 480 min, it is possible that there may be persistent contrast opacification owing to sequestration of the agent in inflammatory cells, such as macrophages. It is worth noting that inherent error associated with SNR analysis of plaque should be taken into account

and the observed PS-dependent enhancement is statistically significant, yet somewhat small (Fig. 6C).

A number of studies in experimental models of atherosclerosis and human studies have demonstrated the critical importance of recognizing macrophage content within plaque. The extent of macrophage infiltration is directly correlated to subsequent complications associated with plaque disruption (20). Previous approaches that have focused on macrophage imaging using MRI approaches have sought to recognize specific receptors on macrophage surface, such as the scavenger receptors (6, 7) or other antigenic determinants associated with oxidative modification of lipoproteins (20). In contrast, our approach seeks to take advantage of a specific high-efficiency endogenous mechanisms by which macrophages engulf apoptotic cells and do not depend on antigen-antibody interactions to deliver Gd. Based on our data, we now demonstrate significant vascular wall enhancement that persists many hours after contrast material injection. These findings suggest that simple modification of existing Gd-containing contrast agents could render them as lesion-specific targeted contrast agents. Such an approach will not involve the use of antibodies or other targeting methods that are not clinically approved and moreover require the usage of PEG protection. Previous reports using PS-containing liposomes incorporated PEG chains grafted on to the liposome and/or micelle surface (6–8). While the incorporation of PEG has a beneficial impact on prolonging circulation times and in enhancing intravascular signal characteristics when administered in vivo, it may have other unintended consequences (9, 21, 22). Specifically, the existence of a PEG-mediated shield effect has been described previously and has been theorized to hamper or abort targeted interaction of the carrier/vector to the antigenic determinants by blocking sites of recognition. Therefore, in our approach, we deliberately avoided PEG as our intent was to optimize delivery to a specific population of cells. Our data seem to indicate prolonged vascular retention for several hours after administration and may represent an incremental advance over current formulations used clinically that have minimal effects on wall enhancement or effects that are transient (<1 h).

In conclusion, liposomes containing PS may represent a novel approach to target macrophages in the atherosclerosis. Further modifications to enhance uptake and retention times may represent a simple and clinically relevant strategy to image atherosclerosis as phospholipid formulations are widely used clinically and may not pose undue concerns with regards to safety.⬛

REFERENCES

1. Wickline, S. A., A. M. Neubauer, P. M. Winter, S. D. Caruthers, and G. M. Lanza. 2007. Molecular imaging and therapy of atherosclerosis with targeted nanoparticles. *J. Magn. Reson. Imaging.* **25:** 667–680.

2. Jaffer, F. A., P. Libby, and R. Weissleder. 2007. Molecular imaging of cardiovascular disease. *Circulation.* **116:** 1052–1061.

3. Jaffer, F. A., and R. Weissleder. 2005. Molecular imaging in the clinical arena. *JAMA.* **293:** 855–862.

4. Frias, J. C., K. J. Williams, E. A. Fisher, and Z. A. Fayad. 2004. Recombinant HDL-like nanoparticles: a specific contrast agent for MRI of atherosclerotic plaques. *J. Am. Chem. Soc.* **126:** 16316–16317.

5. Corbin, I. R., H. Li, J. Chen, S. Lund-Katz, R. Zhou, J. D. Glickson, and G. Zheng. 2006. Low-density lipoprotein nanoparticles as magnetic resonance imaging contrast agents. *Neoplasia.* **8:** 488–498.

6. Amirbekian, V., M. J. Lipinski, K. C. Briley-Saebo, S. Amirbekian, J. G. S. Aguinaldo, D. B. Weinreb, E. Vucic, J. C. Frias, F. Hyafil, V. Mani, et al. 2007. Detecting and assessing macrophages in vivo to evaluate atherosclerosis noninvasively using molecular MRI. *Proc. Natl. Acad. Sci. USA.* **104:** 961–966.

7. Mulder, W. J. M., G. J. Strijkers, K. C. Briley-Saboe, J. C. Frias, J. G. S. Aguinaldo, E. Vucic, V. Amirbekian, C. Tang, P. T. K. Chin, K. Nicolay, et al. 2007. Molecular imaging of macrophages in atherosclerotic plaques using bimodal PEG-micelles. *Magn. Reson. Med.* **58:** 1164–1170.

8. Mulder, W. J., K. Douma, G. A. Koning, M. A. van Zandvoort, E. Lutgens, M. J. Daemen, K. Nicolay, and G. J. Strijkers. 2006. Liposome-enhanced MRI of neointimal lesions in the ApoE-KO mouse. *Magn. Reson. Med.* **55:** 1170–1174.

9. Sofou, S. 2007. Surface-active liposomes for targeted cancer therapy. *Nanomedicine.* **2:** 711–724.

10. Klibanov, A. L., K. Maruyama, A. M. Beckerleg, V. P. Torchilin, and L. Huang. 1991. Activity of amphipathic poly(ethylene glycol) 5000 to prolong the circulation time of liposomes depends on the liposome size and is unfavorable for immunoliposome binding to target. *Biochim. Biophys. Acta.* **1062:** 142–148.

11. Henson, P. M., D. L. Bratton, and V. A. Fadok. 2001. Apoptotic cell removal. *Curr. Biol.* **11:** R795–R805.

12. Tait, J. F., and C. Smith. 1999. Phosphatidylserine receptors: role of CD36 in binding of anionic phospholipid vesicles to monocytic cells. *J. Biol. Chem.* **274:** 3048–3054.

13. Prosser, R. S., H. Bryant, R. G. Bryant, and R. R. Vold. 1999. Lanthanide chelates as bilayer alignment tools in NMR studies of membrane-associated peptides. *J. Magn. Reson.* **141:** 256–260.

14. Kabalka, G. W., M. A. Davis, T. H. Moss, E. Buonocore, K. Hubner, E. Holmberg, K. Maruyama, and L. Huang. 1991. Gadolinium-labeled liposomes containing various amphiphilic Gd-DTPA derivatives: targeted MRI contrast enhancement agents for the liver. *Magn. Reson. Med.* **19:** 406–415.

15. Stewart, J. C. 1980. Colorimetric determination of phospholipids with ammonium ferrothiocyanate. *Anal. Biochem.* **104:** 10–14.

16. National Institutes of Health. 1985. Guide for the Care and Use of Laboratory Animals. NIH Publication No. 86–23, revised 1985. NIH, Washington, DC.

17. Bogaert, J. S. D., and A. M. Taylor. 2005. Clinical Cardiac MRI. Springer, New York.

18. Ravichandran, K. S., and U. Lorenz. 2007. Engulfment of apoptotic cells: signals for a good meal. *Nat. Rev. Immunol.* **7:** 964–974.

19. Huynh, M. L. N., V. A. Fadok, and P. M. Henson. 2002. Phosphatidylserine-dependent ingestion of apoptotic cells promotes TGF-beta 1 secretion and the resolution of inflammation. *J. Clin. Invest.* **109:** 41–50.

20. Briley-Saebo, K. C., P. X. Shaw, W. J. Mulder, S. H. Choi, E. Vucic, J. G. Aguinaldo, J. L. Witztum, V. Fuster, S. Tsimikas, and Z. A. Fayad. 2008. Targeted molecular probes for imaging atherosclerotic lesions with magnetic resonance using antibodies that recognize oxidation-specific epitopes. Circulation **117:** 3206–3215.

21. Photos, P. J., L. Bacakova, B. Discher, F. S. Bates, and D. E. Discher. 2003. Polymer vesicles in vivo: correlations with PEG molecular weight. *J. Control. Release.* **90:** 323–334.

22. Maruyama, K., T. Yuda, A. Okamoto, S. Kojima, A. Suginaka, and M. Iwatsuru. 1992. Prolonged circulation time in vivo of large unilamellar liposomes composed of distearoyl phosphatidylcholine and cholesterol containing amphipathic poly(ethylene glycol). *Biochim. Biophys. Acta.* **1128:** 44–49.